

Computational Modelling of the Mechanics of Trabecular Bone and Marrow Using Fluid Structure Interaction Techniques

E. BIRMINGHAM,¹ J. A. GROGAN,¹ G. L. NIEBUR,² L. M. MCNAMARA,¹ and P. E. MCHUGH¹

¹Biomechanics Research Centre (BMEC), Mechanical and Biomedical Engineering, College of Engineering and Informatics, National University of Ireland Galway, Galway, Ireland; and ²Department of Aerospace and Mechanical Engineering, University of Notre Dame, Notre Dame, IN 46556, USA

(Received 31 July 2012; accepted 26 November 2012; published online 4 December 2012)

Associate Editor Sean S. Kohles oversaw the review of this article.

Abstract—Bone marrow found within the porous structure of trabecular bone provides a specialized environment for numerous cell types, including mesenchymal stem cells (MSCs). Studies have sought to characterize the mechanical environment imposed on MSCs, however, a particular challenge is that marrow displays the characteristics of a fluid, while surrounded by bone that is subject to deformation, and previous experimental and computational studies have been unable to fully capture the resulting complex mechanical environment. The objective of this study was to develop a fluid structure interaction (FSI) model of trabecular bone and marrow to predict the mechanical environment of MSCs *in vivo* and to examine how this environment changes during osteoporosis. An idealized repeating unit was used to compare FSI techniques to a computational fluid dynamics only approach. These techniques were used to determine the effect of lower bone mass and different marrow viscosities, representative of osteoporosis, on the shear stress generated within bone marrow. Results report that shear stresses generated within bone marrow under physiological loading conditions are within the range known to stimulate a mechanobiological response in MSCs *in vitro*. Additionally, lower bone mass leads to an increase in the shear stress generated within the marrow, while a decrease in bone marrow viscosity reduces this generated shear stress.

Keywords—Bone, Bone marrow, Fluid structure interaction, Computational fluid dynamics, Shear stress, Mesenchymal stem cells, Osteoporosis, Mechanobiology.

INTRODUCTION

Mesenchymal stem cells (MSCs) are multi-potent cells capable of forming tissues such as bone, cartilage

and fat. This makes them attractive candidates for tissue engineering applications. The unique native micro-environment in which MSCs reside within the bone marrow of trabecular bone is known as a stem cell niche for MSCs. While the stem cell niche was first identified for hematopoietic stem cells within bone marrow, it also contains and supports MSCs.²⁷ Schofield identified a niche as having three main functions: (1) maintaining MSC quiescence, (2) promoting cell number and (3) directing differentiation.⁴⁵ Although studies have mainly sought to understand the role of paracrine signalling from cells within the niche^{3,18,50} MSCs are known to be mechano-sensitive and there is increasing evidence that the mechanical environment imposed within the niche also plays an important role in the functions of the niche.^{10,17,22,38} Furthermore, mechanical loading has been used to direct MSCs to differentiate *in vitro*^{1,9} and as such the mechanical stimulus to cells has important implications for bone tissue engineering and regeneration applications. However to date the precise mechanical environment of bone marrow MSCs *in vivo* remains unclear and an improved understanding is needed to fully determine the role of mechanical signals on MSC differentiation.

Trabecular bone is a porous structure located at the end of long bones, in irregular shaped bones such as the sternum, the skull and in the vertebral bodies of the spine. The red bone marrow found within the pores acts as a home for a host of different cells including hematopoietic progenitors and their progeny including blood cells, immune cells, and osteoclasts, and MSCs and their progeny including fibroblasts, endothelial cells, adipocytes and osteoblasts.²⁷ These cells and the extracellular matrix they produce make up the composition of marrow. The mechanical environment of

Address correspondence to E. Birmingham, Biomechanics Research Centre (BMEC), Mechanical and Biomedical Engineering, College of Engineering and Informatics, National University of Ireland Galway, Galway, Ireland. Electronic mail: e.birmingham1@nuigalway.ie

trabecular bone marrow remains poorly characterized.²³ Previous studies have focused on the possible role for bone marrow in the hydraulic stiffening of bone.^{7,35,36} However, there has been little insight into the mechanical environment of the marrow and how this alters during physiological loading, or with diseases such as osteoporosis, which is critical in understanding the loading experienced by MSCs *in vivo*. Investigations into the mechanical properties of bone marrow have revealed it to be a highly viscous fluid⁵ while also displaying viscoelastic solid properties.⁵⁶ Experimental studies have shown that loading of bone induces pressure gradients within the marrow, known as the intramedullary pressure.^{15,39,41} Such pressure gradients likely cause flow of the marrow, generating shear stresses, thus providing a possible stimulus for the osteogenic differentiation of MSCs *in vivo*.²³

The composition of bone marrow varies greatly with age and location, and in particular the bone marrow becomes increasingly fatty with age.^{30,49} A high fat content in bone marrow is also associated with diseases such as osteoporosis^{43,54}; this change in marrow composition is accompanied by the decrease in bone mass, characteristic of the disease. Furthermore, a decrease in osteogenic differentiation of MSCs is coupled with an increase in adipogenic differentiation of MSCs, which might suggest that stem cell differentiation plays a crucial role in osteoporosis.^{13,43} As the changes in marrow composition (i.e. higher fat content) and decrease in bone mass alter the mechanical environment, it is possible that such changes will directly influence the mechanical stimulation experienced by MSCs *in vivo*. Moreover, it is also possible that the increased adipocyte content of the marrow contributes to the pathogenesis of the bone¹¹ due to marrow adipocytes actively recruiting osteoclasts.⁵¹ However the role of changes in marrow composition and bone mass on the mechanical environment experienced by MSCs in the bone marrow have never been investigated.

The objective of this study is to examine the complex multiphysics mechanical environment of bone marrow using computational models that capture the interaction of the bone and marrow during typical loading. A novel fluid structure interaction (FSI) approach is used to predict the mechanical environment of the stem cell niche and how this environment alters during osteoporosis. These FSI models extend the results from previous approaches which have modelled the bone as rigid,^{12,37,47} the marrow as a soft solid⁵⁵ or used a continuum approach to describe marrow shear stress coupled to bone deformation.¹⁴ A 3D periodic unit cell approach is used to generate models of trabecular bone and marrow, with an idealized trabecular geometry. In a first step, to validate

the idealized model geometry approach, models are used to predict trabecular bone permeability and are compared to experimental data. Following on from this, the most appropriate boundary conditions are determined for FSI simulations using the periodic unit cell approach and results are compared to a computational fluid dynamics (CFD) only approach. Subsequently, the models are used to determine how a decreasing bone mass and a change in viscosity can influence the *in vivo* mechanical stimulation of MSCs. In this way the study generates insight into how the mechanical environment of MSCs changes during osteoporosis.

MATERIALS AND METHODS

Validation Study: Predicting Permeability

An idealized structure of trabecular bone was used (Fig. 1a) representing a number of individual trabeculae. A unit size of 1.25 mm was selected in order to provide a pore size of in the scale of 1 mm based on representative values for trabecular bone.²⁶ The marrow (fluid) structure was established as the exact inverse of the bone shape (Fig. 1b). The solid structure was created in Abaqus Explicit (version 6.11) with the fluid domain created in Abaqus CFD (version 6.11). To validate the approach for modelling trabecular bone marrow, CFD models were generated to predict the permeability of trabecular bone for comparison to experimental measurements of trabecular bone permeability. The aim of this validation was to demonstrate that the model framework can generate experimentally accurate permeabilities indicating the suitability of the idealized geometries. Specifically, based on prescribed inlet velocities, ranging from 0.1 to 5 mm/s, flow through the structure was simulated and the pressure differential was obtained from the output

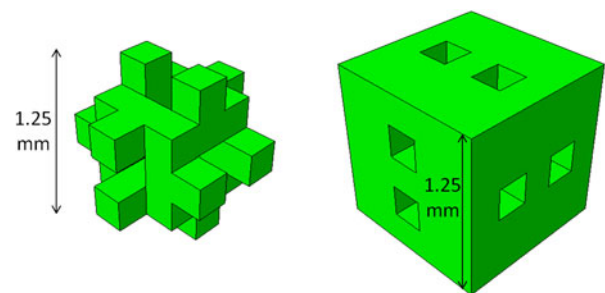


FIGURE 1. Idealized repeating unit of (a) bone and (b) marrow, based on previously used geometries,^{19,55} where the marrow structure is the inverse of the bone. Dimensions are taken in order to provide a pore size of approximately 1 mm.²⁶ Bone struts are increased or decreased to achieve different BV/TV percentages while retaining the same overall unit size of 1.25 mm.

to determine the permeability of the structure through the use of Darcy's law (Eq. (1)),

$$U_D = \frac{Q}{A_S} = \left(\frac{k}{\mu}\right) \frac{P_U - P_D}{L_S} \quad (1)$$

where U_D is the Darcy's velocity, Q is the volume flow rate, A_S is the cross-sectional area of the model, k is the permeability, μ is the viscosity (viscosity of water 1 mPa s), P_U is the upstream pressure, P_D is the downstream pressure (Fig. 2) and L_S is the length of the bone unit in the region of interest (Fig. 1, 1.25 mm). The models were formulated to be representative of the experimental conditions reported in Nauman *et al.*,³³ with the bone modelled as rigid for these permeability studies and the flow modelled as incompressible. The boundary between the solid and the fluid was defined as a no slip boundary where the velocity of the fluid at the boundary is equal to the velocity of the solid.

FSI Model Formulation

In order to model the uni-axial compression of a repeating unit of idealized trabecular bone, symmetry boundary conditions must be used ensuring all sides remain orthogonal before and after loading.³² It is important to note that due to the material and loading directions symmetries in these analyses, the general periodic boundary conditions that normally apply for periodic unit cell analyses reduce to the simpler symmetry boundary conditions as implemented here.⁴ To achieve this repeating unit approach within the fluid domain during FSI analyses a combination of different boundary conditions were analysed and compared as described below.

Four different cases were considered to derive the most appropriate fluid boundary conditions, as the movement of fluid through bone marrow cavities of bone is not well understood. In the first case a CFD-only analysis consisting of a velocity driven marrow flow past rigid bone was modelled (CFD-only, Fig. 3a). This inlet velocity, $Vi = 0.00375$ mm/s was equivalent to a strain rate of 3000 $\mu\epsilon/s$ and was applied using a smooth ramp of an amplitude between 0 and 1 at 1 Hz for 3 cycles. Flow was modelled as symmetric in the X and Z directions by preventing velocity normal to the respective boundaries and a zero pressure outlet was applied on the bottom surface.

In the second case, a marrow flow, driven by the elastic compression of the bone was introduced (FSI-P, Fig. 3b). A displacement representing 3000 $\mu\epsilon$ compressive strain (applied using a smooth ramp of an amplitude between 0 and 1 at 1 Hz for 3 cycles) was applied through the use of a "soft cap" (Young's

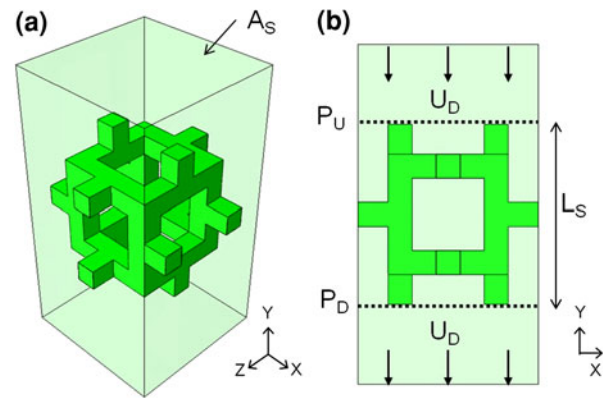


FIGURE 2. Idealized trabecular bone in marrow displaying elongated inlet and outlet for permeability study and Darcy's Law parameters representing the experimental study by Nauman *et al.*,³³ (a) iso-view and (b) plane view.

modulus (E) of 15 MPa), connected to the bone ($E = 15$ GPa). This "soft cap" was necessary in order to implement the required boundary conditions due to restrictions in coupling nodes between the fluid and solid meshes within Abaqus. The prescribed displacement was applied to a master node and all other nodes on the inside/bottom surface of the cap were constrained to move together with the master node in the y -direction, using an equation constraint. No constraint was applied to these nodes in the X and Z directions. These boundary conditions, combined with the fact that the cap was of negligible stiffness relative to the bone, ensured that the marrow and bone domains moved as one without constraining the bone struts on the top surface in the X and Z directions. Fluid velocity was again prevented out of plane in the X and Z directions on the respective boundaries with a zero pressure condition on the bottom surface. Symmetry deformation constraints were applied to the solid bone struts on the X and Z surfaces, again using an equation constraint. This coupled the displacements of all nodes on the given strut faces to a master node, for displacement components in the direction normal to the respective face. This ensured the sides of the solid bone remain orthogonal during loading, but could displace in the X and Z directions.

In the third case the solid boundary conditions remained the same as FSI-P but the fluid velocity was set to zero normal to the plane of the bottom boundary (FSI-Y, Fig. 3c). This allowed for symmetric fluid flow conditions on all planes, ensuring the fluid remained within the volume when compressed, while allowing the displacement of the fluid domain boundaries which caused the fluid itself to displace accordingly.

While cases FSI-P and FSI-Y implement symmetry of fluid velocity on the boundaries they do not implement symmetry deformation conditions to the fluid

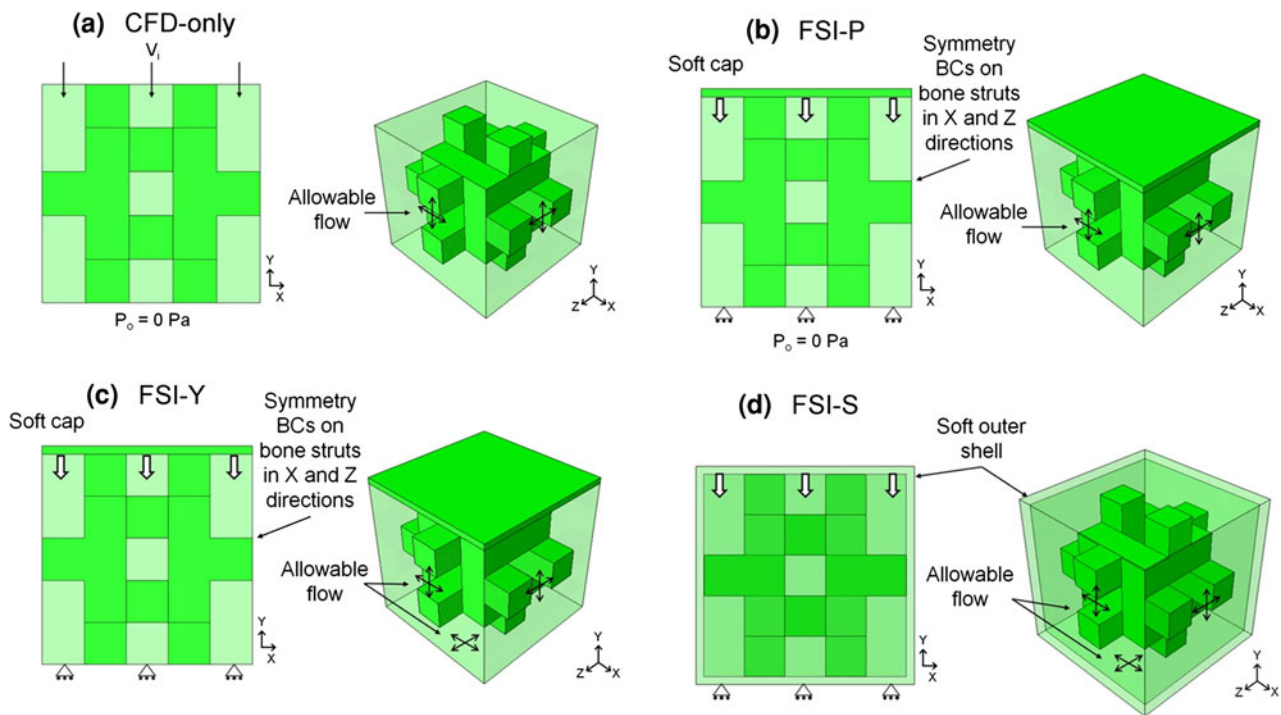


FIGURE 3. (a) CFD-only, velocity driven flow of the marrow past a rigid bone, flow was modelled as symmetric in the X and Z directions with a zero pressure outlet. (b) FSI-P, marrow flow driven by the elastic compression of the bone (achieved with a soft cap) with symmetry fluid flow conditions on the X and Z planes and a zero pressure outlet. Symmetry deformation constraints were applied to the bone struts on the X and Z surfaces, which coupled the displacements, in the direction normal to the respective faces, of all nodes on the respective strut faces to a master node, for displacement components in the direction normal to that face. (c) FSI-Y, same as FSI-P except flow was prevented out of plane on the bottom surface. (d) FSI-S, symmetry deformation constraints were applied to the boundaries of the fluid domain through the use of a soft outer shell; this is used to explicitly constrain the unit cell boundary both fluid and solid to remain cuboidal during deformation, by coupling the displacements, in the direction normal to the respective faces, of all nodes to a master node on the inside surface.

domain mesh. This was achieved in the final analysis, FSI-S, which used the same fluid conditions as FSI-Y but a soft ($E = 15$ MPa) outer shell was also included. This explicitly constrained the unit cell boundary, both fluid and solid, to remain cuboidal during deformation, and therefore is a full implementation of symmetry boundary conditions. The constraint was achieved by coupling the displacements, in the direction normal to the respective faces, of all nodes to a master node on the inside surface (FSI-S, Fig. 3d).

Marrow was modelled as an incompressible, Newtonian fluid using the experimental results of Bryant *et al.*⁵ with a viscosity of 0.4 Pa s. For the FSI analyses bone was modelled as a linear elastic material ($E = 15$ GPa, $\nu = 0.3$).²⁶ A no slip boundary was applied at the interface between the marrow and the bone.

The solid and fluid analyses were fully coupled using the Abaqus co-simulation engine (Gauss–Seidel coupling algorithm), allowing for a two-way coupled FSI.¹⁶ The equations for the solid and fluid models are solved separately, and loads and boundary conditions are exchanged at the interface region. Fluid flow is modelled in an Eulerian domain employing the Arbitrary Lagrangian–Eulerian (ALE) method which is

used when the boundaries of the Eulerian domain are moving due to FSI.¹⁶

This ALE formulation allows for mesh deformation of the fluid domain, therefore, it was deemed that FSI-S is the most appropriate approach to simulate *in vivo* loading conditions, using a periodic unit cell approach. This approach, which ensures that the fluid domain sides remain orthogonal during loading (matching the solid deformation conditions), is used in the subsequent analyses in this study.

The Mechanical Environment of Bone Marrow During Osteoporosis

Different bone masses or BV/TV (Bone Volume/Tissue Volume) percentages of 11.06, 15.10, 18.02, 25.60 and 29.40% were examined to determine the effect of bone mass on the velocity and shear stress generated within the marrow due to mechanical loading. Different BV/TV percentages were achieved in the solid model by creating parts with different bone strut widths while maintaining the overall unit size of 1.25 mm. A Boolean cut was then performed using the solid part to create the fluid part. Percentages were

selected as a range of BV/TV from osteoporotic (11.06%) to healthy bone (29.40%).²⁴ A force controlled compression of 3 N (which generates strains typical of physiological loading in the 29.40% model⁶) and a displacement controlled compression of 3000 μe were examined for each BV/TV. Boundary conditions were maintained as shown in Fig. 3d, as already mentioned this is a full implementation of symmetry boundary conditions and was deemed most appropriate following the initial FSI model formulation study. Different marrow viscosities were also examined as osteoporotic bone is usually accompanied by a fattier marrow, which impacts on the marrow viscosity.⁴³

Within Abaqus CFD version 6.11 shear stresses are not outputted directly. To determine the stresses within the current analyses the following approach was used. Firstly, \mathbf{D} is the strain rate tensor, equal to $\frac{1}{2}(\nabla\mathbf{u} + (\nabla\mathbf{u})^T)$, where $\nabla\mathbf{u}$ is the velocity gradient tensor. From this, the scalar shear rate ($\dot{\gamma}$) was calculated as $(2\text{tr}(\mathbf{D}\mathbf{D}))^{\frac{1}{2}}$, which can be explicitly written as follows:

$$\dot{\gamma} = \left[2 \left\{ \left(\frac{\partial u}{\partial x} \right)^2 + \left(\frac{\partial v}{\partial y} \right)^2 + \left(\frac{\partial w}{\partial z} \right)^2 \right\} + \left(\frac{\partial u}{\partial y} + \frac{\partial v}{\partial x} \right)^2 + \left(\frac{\partial u}{\partial z} + \frac{\partial w}{\partial x} \right)^2 + \left(\frac{\partial v}{\partial z} + \frac{\partial w}{\partial y} \right)^2 \right]^{\frac{1}{2}} \quad (2)$$

where u , v and w are the velocities in the x , y and z directions respectively. For a viscous fluid, the energy dissipated in flow is given by the viscous-dissipation function Φ .⁵²

$$\Phi = \mu\dot{\gamma}^2 \quad (3)$$

where μ is the viscosity of the marrow. In the present work a shear stress τ is calculated using the basic Newtonian viscous flow law $\tau = \mu\dot{\gamma}$. The rate of work done per unit volume by this stress, $\tau\dot{\gamma}$, equals the viscous dissipation, through Eq. (4). τ is then used to characterize the shear stress state in the marrow. This was implemented using a Python script which inputted the velocities and co-ordinates at each node from Abaqus output file.

For the models in the FSI formulation study and the subsequent osteoporosis studies, the solid bone domain consisted of 8-node brick elements (C3D8R), with element numbers in the range of 63,348 to 76,656. The fluid domain consisted of 8-node brick fluid elements (FC3D8), with element numbers in the range of 93,000–116,407. These mesh densities were arrived at as a result of a mesh convergence study for the different BV/TV percentages examined, as these necessitate a change in the model geometry, resulting

in a square element length of approximately 0.025 mm in all analyses. Material properties in the different BV/TV models were maintained as outlined in the FSI model formulation methods. A value of 0.4 Pa s for the marrow viscosity was taken for the majority of this study in accordance with the study by Bryant *et al.*,⁵ Values of 1 Pa s and 0.1 Pa s were also examined as these represent the upper and lower values reported from experiments.^{23,56}

The Reynolds number (Re) was calculated for all analyses to determine the relative influence of viscous and inertial forces (Eq. (2)).

$$\text{Re} = \frac{\rho V d}{\mu} \quad (4)$$

In this equation the trabecular spacing was used as the characteristic dimension (d), the density (ρ) was taken from White *et al.*,⁵³ with a value of 1.06 kg m⁻³, the viscosity (μ) was taken from Bryant *et al.*⁵ as previously stated and the average velocity (V) was determined at the peak point of the cycle. For Reynolds numbers of less than 1, viscous forces dominate, and the flow is laminar.

RESULTS

Validation Study: Predicting Permeability

The permeability simulations were performed for the above mentioned range of BV/TV percentages (11.06, 15.10, 18.02, 25.60 and 29.40%) and Darcy's Law was used to extract the permeabilities. They varied between $6.82 \times 10^{-10} \text{ m}^2$ to $1.95 \times 10^{-9} \text{ m}^2$ decreasing with greater bone volume fraction as expected (Fig. 4a). Values found were within reported values of permeability for trabecular bone for experimental^{21,33} and computational studies^{12,47} (Fig. 4b). This result gives confidence that assumed idealized geometry is sufficiently representative to study the mechanics of the bone and marrow interaction at this size scale.

FSI Model Formulation

The simulations were run for 3 cycles, however changes from cycle to cycle were negligible, showing that transient effects could be ignored. Based on this, the results presented below are for the first cycle. The velocity profile within the marrow was found to differ greatly between velocity driven flow of the CFD-only analysis and the marrow flow driven by bone compression achieved with the application of a FSI interaction (Fig. 5a vs. Figs. 5b–5d). The Reynolds numbers for all analyses were much less than 1 showing

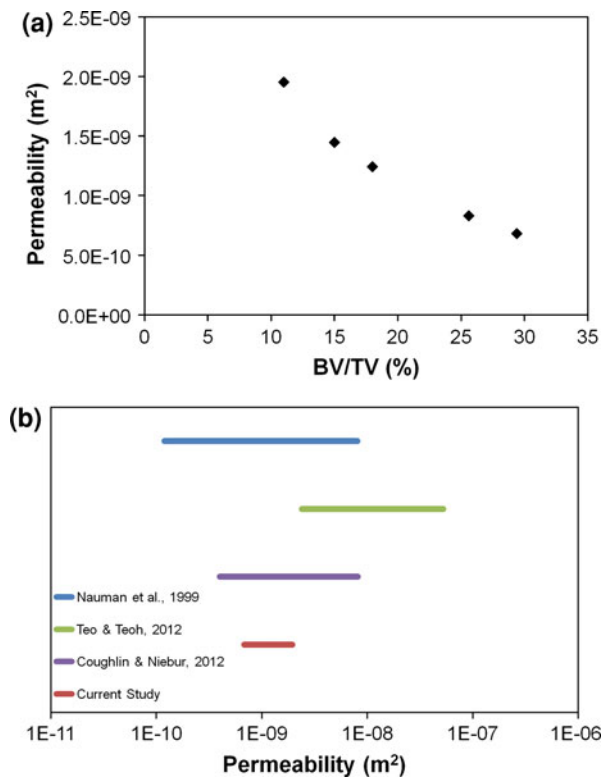


FIGURE 4. (a) Values of permeability calculated for BV/TV percentages of 11.06, 15.10, 18.02, 25.60 and 29.40% and (b) comparison of permeability results for the current study, experimental studies^{21,33} and computational studies.^{12,47}

that the viscous forces are dominating these analyses and that the assumption of laminar flow is appropriate, see Fig. 5.

Velocities and shear stresses in the fluid were examined at the peak overall velocity point of the cycle, i.e. at 0.5 s, while the displacements and stresses in the solid were examined at the peak overall displacement point, i.e. at 1 s. The statistical distribution of velocity within the marrow (Fig. 5e) reveals that the maximum velocities in the CFD-only analysis were over twice as large as those of the FSI analyses (0.0191 mm/s compared to 0.0072 mm/s for the FSI-P, 0.0072 for the FSI-Y and 0.00771 mm/s for the FSI-S). Similarly high values were found for the 90th percentile demonstrating that 10% of the nodal velocity values are much higher in the CFD-only analysis compared to the FSI analyses. When the 70th percentile of the velocity was examined in the marrow the four different boundary conditions were found to be much more comparable. While this demonstrates that 70% of the nodal velocities in all the analyses are within a small range, the CFD-only analysis still predicts high peak velocity values relative to the other cases. The FSI-Y analysis predicted on average the lowest velocities. The FSI analysis with symmetry conditions (FSI-S)

predicted the most homogenous distribution of velocity within the marrow.

Examining the stresses and strains generated in the bone for the different fluid boundary conditions in the FSI analyses (see Table 1) reveals that the introduction of a soft outer cap/case in order to apply symmetry boundary conditions to the fluid domain does not interfere with the bone deformation and motion while it does alter the shear stress generated within the marrow.

The Mechanical Environment of Bone Marrow During Osteoporosis

The influence of different bone volume fractions was examined by employing both force and displacement controlled compression. With an applied force of 3 N it was found that a lower BV/TV percentage resulted in an increased velocity within the marrow as evident when the velocity distributions are examined using a histogram (see Fig. 6a). The majority of the nodal velocities (70%) predicted for the 11.06% BV/TV were found to be greater than 0.01 mm/s whereas for the other bone volumes examined (15.10, 18.02, 25.60 and 29.40%) the majority of the nodal velocities were in the range of 0–0.001 mm/s. The velocity profile for the 11.06% BV/TV can be seen in Fig. 6b. The maximum and 90th percentile shear stresses, calculated as described above, were found to decrease by a factor of 10 from the lowest (11.06%) and the highest BV/TV (29.40%) examined here (Fig. 6c). The shear stress generated within the marrow due a 3 N load is shown in Fig. 6d for a BV/TV of 11.06%. In contrast, when the velocity distribution was examined for a strain controlled compression (3000 $\mu\epsilon$) no difference in the average velocities was observed for any of the different bone volume fractions investigated (Fig. 7).

The influence of the different viscosities can be seen by examining the shear stresses generated within the marrow (Fig. 8a), however changing the viscosity of the bone marrow was found to have no significant effect on the average velocity within the bone marrow (Fig. 8b). Figure 8c reveals that the relationship between shear stress and BV/TV is not completely linear for any of the viscosities examined ($R^2 = 0.831$ for 0.1 Pa s, $R^2 = 0.844$ for 0.4 Pa s and $R^2 = 0.867$ for 1.0 Pa s). Figure 8d illustrates the proportional relationship between shear stress and viscosity for two of the BV/TV percentages examined (15.10 and 25.60%).

DISCUSSION

In this study a novel FSI approach has been used to predict the mechanical environment (marrow velocity

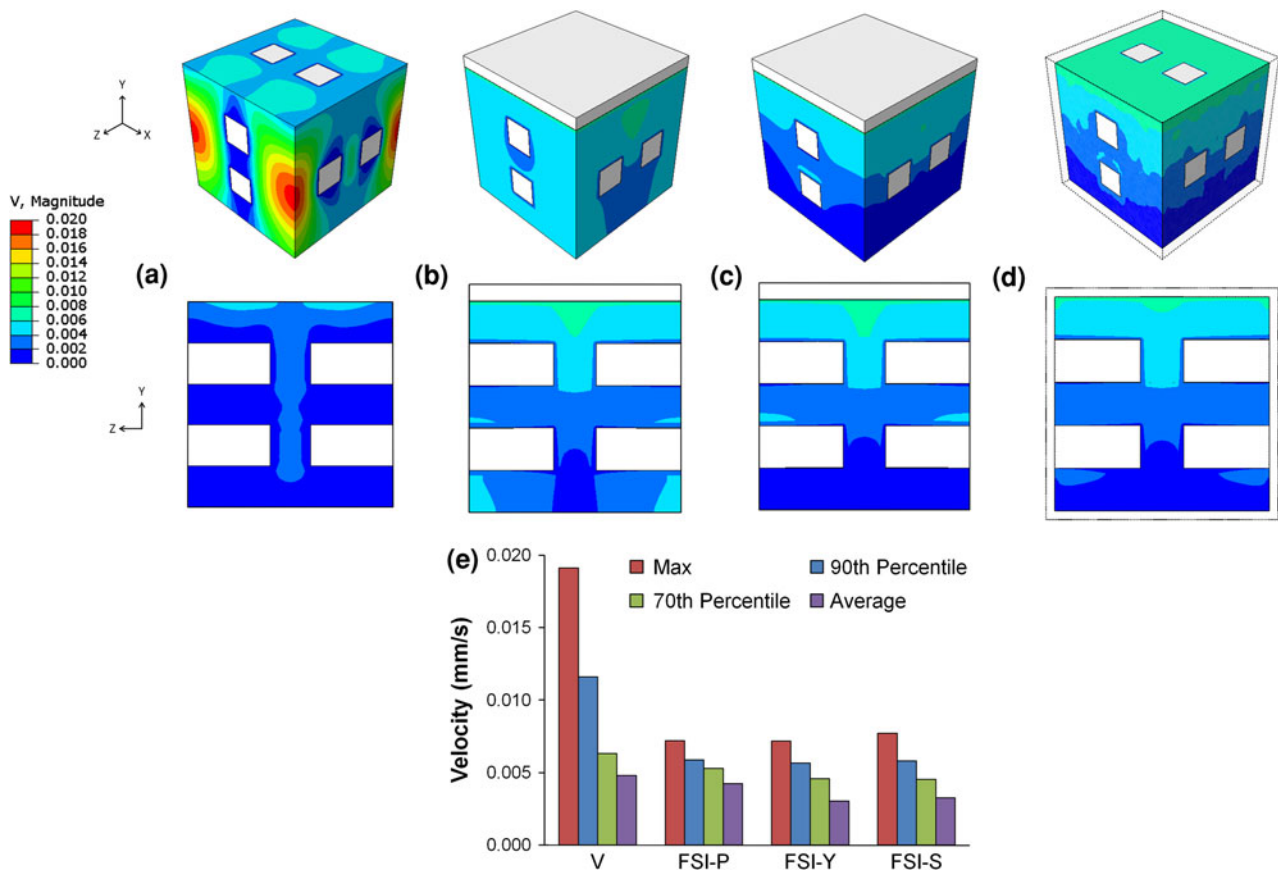


FIGURE 5. Velocity profiles generated within the marrow for (a) velocity only analysis of flow past a rigid bone (V) with a Reynolds number of 0.0032, (b) compression driven marrow flow achieved with the introduction of FSI (FSI-P) with a Reynolds number of 0.0028, (c) FSI compression driven marrow flow with flow constrained within the marrow domain (FSI-Y) with a Reynolds number of 0.0020 and (d) FSI compression driven marrow flow with flow constrained within the marrow domain and symmetry boundary conditions applied to the marrow domain with the use of a soft outer case (FSI-S) with a Reynolds number of 0.0022. Units = mm/s. (e) Statistical distribution of velocity generated within the marrow for the four boundary conditions examined at peak velocity point in cycle (0.5 s). Where the 70th and 90th percentiles are the values of velocity below which 70 and 90% (respectively) of the nodal values fall.

TABLE 1. Stress and strain generated within the bone for a displacement representing $3000 \mu\epsilon$ compressive strain, and resulting shear stress generated within the marrow, examining the influence of the different boundary conditions on the fluid domain during the FSI analyses.

	FSI-P	FSI-Y	FSI-S
Von mises stress (MPa)			
Maximum	69.31	69.31	72.09
Average	18.42	18.42	18.34
Max principal strain ($\mu\epsilon$)			
Maximum	2996.24	2996.24	2990.18
Average	566.00	566.00	562.95
Shear stress (mPa)			
Maximum	66.63	65.35	62.15
Average	6.61	7.94	7.55

and shear stress) experienced within trabecular bone marrow under physiological loading conditions. Velocities generated within the marrow were found to depend on the boundary conditions applied to the fluid, indicating the significance of the correct

boundary selection for FSI investigations. However, the greatest difference was found between the CFD only analysis and the FSI analyses demonstrating the importance of the deformation and motion of the solid bone on marrow movement during compression.

In terms of BV/TV dependence, it was observed here that a decreasing bone volume, representing osteoporotic bone, leads to increasing velocities and shear stresses within the marrow. Additionally it was found that changing marrow viscosities, also representative of osteoporosis, had little influence on the fluid velocity, although, an increasing viscosity increased the shear stress linearly. These findings have important implications for tissue engineering as researchers try to understand or mimic the natural environment of MSCs for studies *in vitro* and for investigating the mechanisms behind bone loss during the disease of osteoporosis.

The application of FSI techniques to study bone marrow is an advancement over previous approaches

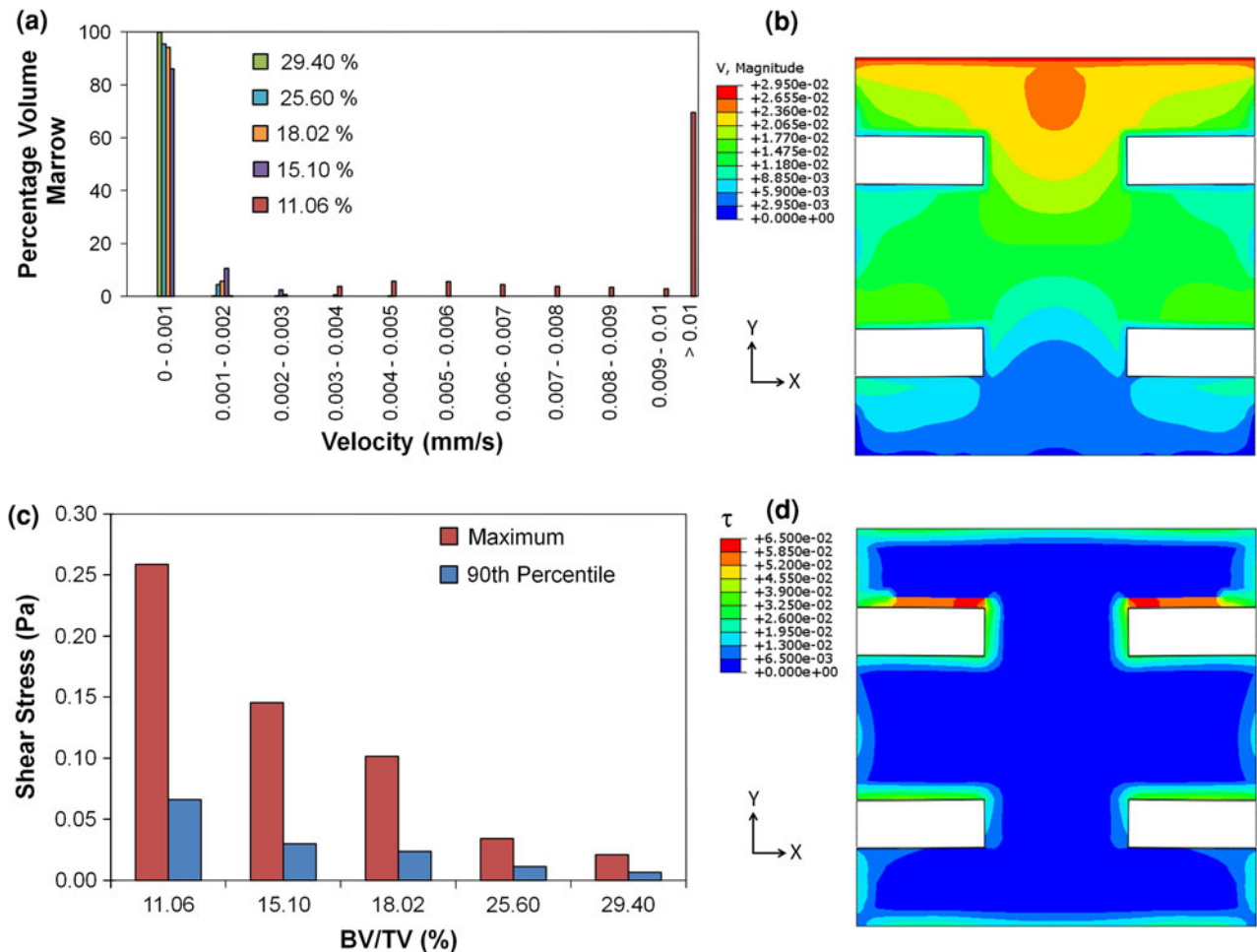


FIGURE 6. (a) Histogram of the velocities within the bone marrow at the peak time of the cycle 0.5 s for the five different bone BV/TV values examined: 11.06, 15.10, 18.02, 25.60 and 29.40%. Velocity values between 0 and 0.01 mm/s are distributed into bins with intervals of 0.001 mm/s to ascertain the statistical distribution of the velocity within the marrow of different bone volume percentages. (b) A velocity contour plot displaying the profile through the marrow of the 11.06% BV/TV sample for a cut through the middle of the marrow in the XY plane (units mm/s). (c) The maximum and 90th percentile value of the shear stress found at the peak time of the cycle for the different bone volume percentages. (d) A shear stress contour plot for the marrow of the 11.06% BV/TV for a cut through the middle of the marrow in the XY plane (units Pa). The 90th percentile is the value of shear stress below which 90% of the element values fall.

where the bone was modelled as rigid with the marrow flowing past it^{37,47} or with the bone marrow modelled as a soft solid.⁵⁵ The CFD-only analysis here was found to produce large peaks in velocities compared to FSI analyses indicating that a CFD-only analysis overestimated the movement of the marrow and as such overestimated the mechanical stimuli experienced by the cells within the marrow. The FSI analysis with the symmetry conditions on the fluid domain (FSI-S) was the most logically representative of the periodic unit cell approach and hence used to examine different BV/TV percentages.

The velocity generated within the marrow was found to be directly dependent on bone volume for a force controlled compression, with the velocity within the marrow decreasing for an increasing BV/TV percentage.

This was as expected as with a decreasing bone volume there is an increasing marrow volume and as such the marrow is experiencing more of the applied load. For a strain controlled compression, where all BV/TV fractions were subjected to the same strain, no difference in marrow velocities was found between the different bone volumes. Again this was as expected as the velocity generated would be the same for the each BV/TV as the displacement is the same.

In vitro, shear stress has been shown to be a regulator of cell differentiation capable of inducing the cell down a osteogenic differentiation pathway.^{1,2,9} A study by Sharpe *et al.*⁴⁶ showed an up regulation of osteoblastic genes such as collagen, osteopontin, osteocalcin and bone sialoprotein in MSCs exposed to fluid shear stress. While the exact method by which cells

convert mechanical stimulation to a biochemical response remains unclear,⁴² mechanoreceptors in the cell surface, such as specific integrins, cadherins, and

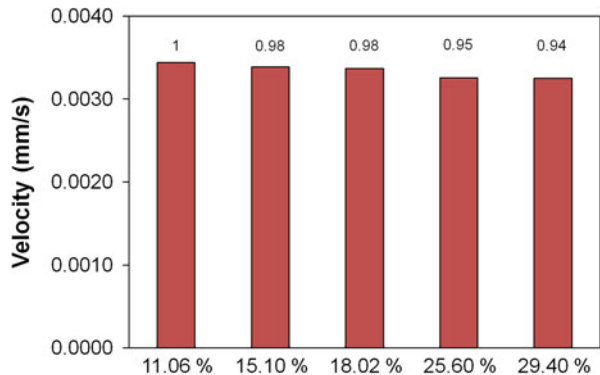


FIGURE 7. Average velocity within the marrow due to a displacement controlled compression of $3000 \mu\text{e}$ (applied using a smooth ramp of an amplitude between 0 and 1 at 1 Hz for 3 cycles) for the five different bone volume percentages examined 11.06, 15.10, 18.02, 25.60 and 29.40%. Values above the bars indicate the results of normalisation of the values to the 11.06% BV/TV result.

calcium channels, play a vital role in the transmission of the mechanical signal into the cell nucleus. This in turn regulates gene expression.²⁹ Additionally, as a result of shear stress, cells can release signalling molecules, such as nitric oxide and prostaglandins, to stimulate neighbouring cells.⁴⁸ Results from the current study can help inform boundary conditions for further computational studies where the focus is on delivering a mechanical stimulation to single cell models³¹ to aid in the understanding of the mechano-transduction process in cells.

The maximum shear stress generated within the marrow (for a viscosity of 0.4 Pa s) for a force controlled compression for the different bone volumes ranged from 0.02 Pa (29.40%) to 0.26 Pa (11.06%). For 2D parallel plate flow chamber experiments shear stress values of 0.1 Pa to 1 Pa have previously been shown to stimulate osteogenic responses in MSCs and pre-osteoblastic cells *in vitro*.^{1,2,9} This suggests that the computational results are predicting shear stresses which are in the lower range of what is needed to stimulate an osteogenic response. However, a separate study which

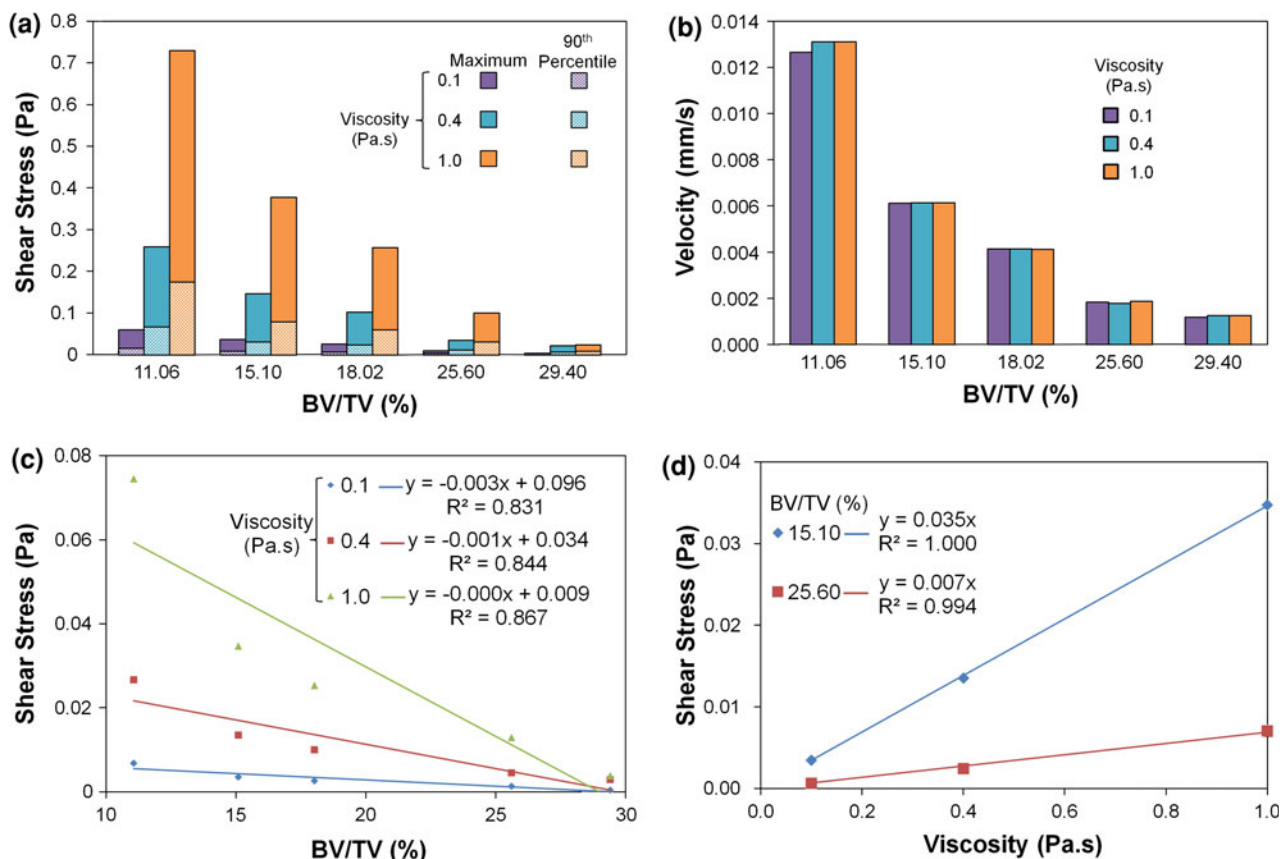


FIGURE 8. (a) The 90th percentile and maximum of the shear stress within the marrow, where the 90th percentile value is represented by a pattern on the maximum solid bar. (b) The average velocity within the marrow at the peak point of the cycle 0.5 s for 3 different viscosities 0.1, 0.4 and 1.0 Pa s, examined within the five BV/TV (Bone Volume/Tissue Volume) percentages. The 90th percentile is the value of shear stress below which 90% of the element values fall. (c) The average shear stress as a function of BV/TV percentage for each viscosity examined and (d) the average shear stress for two of the BV/TV percentages examined as a functions of viscosity. This displays the proportionality of shear stress to viscosity.

examined the effect of applying a 0.06 Pa and 0.6 Pa shear stress found an increased cell proliferation, ALP activity and calcium deposition compared to static controls with no significant differences between the two shear stress values.³⁴ Moreover, Sandino *et al.*, examined the shear stress generated in 3D scaffolds, subjected to a combination of perfusion flow and compression. Values of shear stress were found to range between 0.037 and 0.046 Pa,⁴⁴ which is lower than within a 2D flow chamber. An experimental study by Cartmell *et al.*,⁸ with equivalent inlet velocities and geometries to Sandino *et al.*,⁴⁴ was also found to stimulate the osteogenic differentiation of pre-osteoblastic cells. Taken together, this suggests that in a 3D environment the required shear stress to induce osteogenic differentiation could be lower than what is observed in 2D flow chambers. This implies that 2D studies may not be sufficiently representative of the *in vivo* 3D mechanical environment.

Based on these previous experimental and computational studies, computational results from this investigation indicate that the compression of bone due to physiological loading could generate sufficient shear stress to stimulate the osteogenic differentiation of MSCs with increasing shear stress generated as the BV/TV decreases. However the computational models predict that the 90th percentile shear stress values range from 0.006 Pa (29.40%) to 0.066 Pa (11.06%) indicating that it is only a small percentage of the marrow which experiences sufficient shear stress to stimulate the osteogenic differentiation of MSCs. As such the location of MSCs within the marrow relative to the areas of high shear stress could be crucial in determining osteogenic differentiation in response to bone loading. This would be particularly true in the analysis of realistic geometries where peaks in shear stress may be determined by the geometries and the pores size of the trabecular bone.

Porter *et al.*,³⁷ discussed the difficulties in comparing the response seen in cells exposed to shear stress stimuli in a 2D flow chamber to the response seen in 3D scaffolds.³⁷ The same questions arise when trying to compare a computational model of the *in vivo* structure to *in vitro* experiments. Nonetheless, based on current knowledge, the results of the present study demonstrate that the physiological compression driven flow of the marrow causes sufficiently large shear stress to stimulate osteogenic differentiation of MSCs. Moreover, the results provide shear stress values which could help to interpret and design 3D bone tissue engineering scaffolds which aim to mimic the natural mechanical environment of MSCs.

When the effect of decreasing BV/TV was examined the largest shear stress values were found in the marrow of lower BV/TV percentages. These findings may indicate that MSCs in a lower BV/TV environment

(characteristic of osteoporosis) would experience a greater mechanical stimuli, that would in turn initiate an osteogenic response, than MSCs in a higher BV/TV environment. However, a decreasing BV/TV with osteoporosis is coupled with an increase in the fat content of marrow and as such the viscosity of the marrow might decrease.^{5,56} As shown in Fig. 8 this decrease in viscosity greatly lowers the magnitude of the shear stress experienced in the lower BV/TV models representative of osteoporotic bone. This is in agreement with a previous analytical study by Dickerson *et al.*,¹⁴ which found the viscosity of bone marrow to be a crucial factor in determining the shear stresses generated within the marrow.

These results suggest that the physiological compression of bone could enhance the osteogenic differentiation of MSCs within individuals with lower BV/TV percentages. However, the accompanying decrease in bone marrow viscosity^{54,56} may limit the shear stress experienced by the MSCs. Therefore the viscosity and the BV/TV percentage are linked and to fully determine the relative weight of either parameter a greater knowledge of the relationship between BV/TV and marrow viscosity is required. Moreover, it is likely that the number of undifferentiated MSCs within the marrow would decrease due to the increasing fat content.⁴³ This could perhaps explain why a higher fat content in bone marrow is thought to be a cause of the pathogenesis of bone in osteoporosis^{11,51} as the shear stress within the marrow is decreasing with decreasing viscosity.

To the authors knowledge this is the first time FSI techniques have been used to examine the movement of marrow within trabecular bone, however, there are limitations to this study that should be considered. There exists very little information on the properties of bone marrow and for this reason a Newtonian, incompressible, homogenous fluid was assumed here. A value of 0.4 Pa s⁵ was assumed for the majority of the study however the sensitivity of the models to the viscosity can be seen in Fig. 8 indicating the need for further experimental characterisation. Moreover, the cellular composition of marrow suggests it is heterogeneous in nature and therefore behaves as a non-Newtonian fluid similar to blood.^{5,56} In addition, bone is known to be anisotropic and viscoelastic, whereas this study assumes a linear elastic material which could affect the strain generated within the bone and hence the stimuli experienced within the marrow. Results here show no stiffening effect due to the presence of marrow or the implementation of the different fluid boundary conditions (Table 1). Previous studies have focused on the hydraulic stiffening effects of marrow within the trabecular bone compartments of whole bones with marrow providing additional stiffness to

the overall bone.^{35,36} This effect is not observed in this study due to the micro-mechanical modelling approach. Here the influence of the solid cortical shell is ignored as the structure is idealized as a repeating unit cell of trabecular bone.

While the focus here was on the marrow in trabecular region, where MSCs predominantly reside, the modelling techniques could be adapted to a larger scale model or multiscale model of a long bone structure to determine how loading influences marrow within the diaphyseal regions. Moreover, the modelling techniques could help determine the deformation of bone marrow in cortical bone regions observed in post-menopausal osteopenic women.²⁰ Additionally, the models could be adapted to investigate the effect of frequency and loading rate on the shear stress generated within the marrow. Due to the nature of bone marrow and the nonlinear material properties of bone it is likely that frequency and loading rate are a crucial factor in determining the response. For example, the intramedullary pressure fluctuations caused by muscle stimulation^{25,28,40} could be modelled to determine whether regions of high shear stress within the model correspond to areas of new bone formation.

While the use of idealized geometries is a limitation, this geometry has been found to be suitable in previous studies to give insights into the mechanical behaviour of trabecular bone during loading.^{19,55} The permeability of the idealized structure (for different BV/TV fractions) was found to fall within reported experimental ranges³³ indicating the suitability of these idealized structures. Although the permeability study used a CFD-only boundary condition, which models the bone as rigid, the bone deformation due to flow is thought to be negligible and won't contribute to the overall pressure differential in the fluid which is used to determine the permeability during steady state flow. Due to the symmetry employed in the unit of bone and marrow, the same quantitative results would be obtained for loading in either the *X*, *Y* or *Z* directions for the present models. However, the influence of shear in the *XY* plane, for example, could be modelled using such idealized geometry employed here and would be of interest for future study. Moreover, loading direction would be an important factor to consider in the modelling of anisotropic unit cells or realistic geometries.

In this study FSI techniques were used to investigate the mechanical environment of trabecular bone marrow, providing a new insight into the mechanical stimuli which MSCs are exposed to *in vivo* due to the physiological compression of bone. Computational results from this investigation indicate that the compression of bone due to physiological loading could generate sufficient shear stress to stimulate the osteogenic differentiation of MSCs. These results can help

inform tissue engineering studies which aim to utilize the mechano-sensitivity of MSCs for improved bone tissue engineering applications by providing realistic shear stress values which MSCs experience *in vivo*. Moreover, these results inform how osteoporosis affects the native mechanical environment of MSCs with increasing shear stress generated as the BV/TV decreases. However, with a decreasing viscosity, thought to be representative of a fattier bone marrow (associated with osteoporosis), the shear stress generated within the osteoporotic marrow decreases.

ACKNOWLEDGMENTS

The authors have no conflicts of interest to declare. The authors acknowledge Dr. Nathan Quinlan for very useful discussions. The authors would like to acknowledge funding from the Irish Research Council, under the EMBARK program (E. Birmingham) and the Science Foundation Ireland E.T.S. Walton program 07/W.I./B1806 (G.L. Niebur).

REFERENCES

- ¹Arnsdorf, E. J., P. Tummala, R. Y. Kwon, and C. R. Jacobs. Mechanically induced osteogenic differentiation—the role of RhoA, ROCKII and cytoskeletal dynamics. *J. Cell Sci.* 122:546–553, 2009.
- ²Bakker, A. D., M. Joldersma, J. Klein-Nulend, and E. H. Burger. Interactive effects of PTH and mechanical stress on nitric oxide and PGE2 production by primary mouse osteoblastic cells. *Am. J. Physiol. Endocrinol. Metab.* 285:E608–E613, 2003.
- ³Birmingham, E., G. L. Niebur, P. E. McHugh, G. Shaw, F. P. Barry, and L. M. McNamara. Osteogenic differentiation of mesenchymal stem cells is regulated by osteocyte and osteoblast cells in a simplified bone niche. *Eur. Cell Mater.* 23:13–27, 2012.
- ⁴Böhm, H. J. A short introduction to continuum micromechanics. In: *Mechanics of Microstructured Materials*, edited by H. J. Böhm, editor. Springer-Verlag, 2004, pp. 1–40.
- ⁵Bryant, J. D., T. David, P. H. Gaskell, S. King, and G. Lond. Rheology of bovine bone marrow. *Proc. Inst. Mech. Eng. H* 203:71–75, 1989.
- ⁶Burr, D. B., C. Milgrom, D. Fyhrie, M. Forwood, M. Nyska, A. Finestone, S. Hoshaw, E. Saiag, and A. Simkin. In vivo measurement of human tibial strains during vigorous activity. *Bone* 18:405–410, 1996.
- ⁷Carter, D. R., and W. C. Hayes. The compressive behavior of bone as a two-phase porous structure. *J. Bone Joint Surg. Am.* 59:954–962, 1977.
- ⁸Cartmell, S. H., B. D. Porter, A. J. García, and R. E. Goldberg. Effects of medium perfusion rate on cell-seeded three-dimensional bone constructs in vitro. *Tissue Eng.* 9:1197–1203, 2003.
- ⁹Case, N., B. Sen, J. A. Thomas, M. Styner, Z. Xie, C. R. Jacobs, and J. Rubin. Steady and oscillatory fluid flows produce a similar osteogenic phenotype. *Calcif. Tissue Int.* 88:189–197, 2011.

- ¹⁰Castillo, A. B., and C. R. Jacobs. Mesenchymal stem cell mechanobiology. *Curr. Osteoporos. Rep.* 8:98–104, 2010.
- ¹¹Cohen, A., D. W. Dempster, E. M. Stein, T. L. Nickolas, H. Zhou, D. J. McMahon, R. Müller, T. Kohler, A. Zwahlen, J. M. Lappe, P. Young, R. R. Recker, and E. Shane. Increased marrow adiposity in premenopausal women with idiopathic osteoporosis. *J. Clin. Endocrinol. Metab.* 2012. doi:10.1210/jc.2012-1477.
- ¹²Coughlin, T. R., and G. L. Niebur. Fluid shear stress in trabecular bone marrow due to low-magnitude high-frequency vibration. *J. Biomech.* doi:10.1016/j.jbiomech.2012.06.020.
- ¹³Di Iorgi, N., M. Rosol, S. D. Mittelman, and V. Gilsanz. Reciprocal relation between marrow adiposity and the amount of bone in the axial and appendicular skeleton of young adults. *J. Clin. Endocrinol. Metab.* 93:2281–2286, 2008.
- ¹⁴Dickerson, D. A., E. A. Sander, and E. A. Nauman. Modeling the mechanical consequences of vibratory loading in the vertebral body: microscale effects. *Biomech. Model. Mechanobiol.* 7:191–202, 2008.
- ¹⁵Downey, D. J., P. A. Simkin, and R. Taggart. The effect of compressive loading on intraosseous pressure in the femoral head in vitro. *J. Bone Joint Surg. Am.* 70:871–877, 1988.
- ¹⁶DS SIMULIA. Abaqus 6.11 theory manual. Providence, RI, USA: DS SIMULIA Corp., 2011.
- ¹⁷Estes, B. T., J. M. Gimble, and F. Guilak. Mechanical signals as regulators of stem cell fate. *Curr. Top. Dev. Biol.* 60:91–126, 2004.
- ¹⁸Fuchs, E., T. Tumber, and G. Guasch. Socializing with the neighbors: stem cells and their niche. *Cell* 116:769–778, 2004.
- ¹⁹Gibson, L. J. The mechanical behaviour of cancellous bone. *J. Biomech.* 18:317–328, 1985.
- ²⁰Goldenstein, J., G. Kazakia, and S. Majumdar. In vivo evaluation of the presence of bone marrow in cortical porosity in postmenopausal osteopenic women. *Ann. Biomed. Eng.* 38:235–246, 2010.
- ²¹Grimm, M. J., and J. L. Williams. Measurements of permeability in human calcaneal trabecular bone. *J. Biomech.* 30:743–745, 1997.
- ²²Guilak, F., D. M. Cohen, B. T. Estes, J. M. Gimble, W. Liedtke, and C. S. Chen. Control of stem cell fate by physical interactions with the extracellular matrix. *Cell Stem Cell* 5:17–26, 2009.
- ²³Gurkan, U. A., and O. Akkus. The mechanical environment of bone marrow: a review. *Ann. Biomed. Eng.* 36:1978–1991, 2008.
- ²⁴Hasegawa, K., C. H. Turner, R. R. Recker, E. Wu, and D. B. Burr. Elastic properties of osteoporotic bone measured by scanning acoustic microscopy. *Bone* 16:85–90, 1995.
- ²⁵Hu, M., J. Cheng, and Y.-X. Qin. Dynamic hydraulic flow stimulation on mitigation of trabecular bone loss in a rat functional disuse model. *Bone* 51:819–825, 2012.
- ²⁶Keaveny, T. M., E. F. Morgan, G. L. Niebur, and O. C. Yeh. Biomechanics of trabecular bone. *Annu. Rev. Biomed. Eng.* 3:307–333, 2001.
- ²⁷Kuhn, N. Z., and R. S. Tuan. Regulation of stemness and stem cell niche of mesenchymal stem cells: implications in tumorigenesis and metastasis. *J. Cell. Physiol.* 222:268–277, 2010.
- ²⁸Lam, H., and Y.-X. Qin. The effects of frequency-dependent dynamic muscle stimulation on inhibition of trabecular bone loss in a disuse model. *Bone* 43:1093–1100, 2008.
- ²⁹Liedert, A., D. Kaspar, R. Blakytyn, L. Claes, and A. Ignatius. Signal transduction pathways involved in mechanotransduction in bone cells. *Biochem. Biophys. Res. Commun.* 349:1–5, 2006.
- ³⁰Liney, G. P., C. P. Bernard, D. J. Manton, L. W. Turnbull, and C. M. Langton. Age, gender, and skeletal variation in bone marrow composition: a preliminary study at 3.0 Tesla. *J. Magn. Reson. Imaging* 26:787–793, 2007.
- ³¹Mazzag, B., and A. I. Barakat. The effect of noisy flow on endothelial cell mechanotransduction: a computational study. *Ann. Biomed. Eng.* 39:911–921, 2011.
- ³²Mullins, L. P., J. P. McGarry, M. S. Bruzzi, and P. E. McHugh. Micromechanical modelling of cortical bone. *Comput. Methods Biomech. Biomed. Eng.* 10:159–169, 2007.
- ³³Nauman, E. A., K. E. Fong, and T. M. Keaveny. Dependence of intertrabecular permeability on flow direction and anatomic site. *Ann. Biomed. Eng.* 27:517–524, 1999.
- ³⁴Nauman, E. A., R. L. Satcher, T. M. Keaveny, B. P. Halloran, and D. D. Bikle. Osteoblasts respond to pulsatile fluid flow with short-term increases in PGE2 but no change in mineralization. *J. Appl. Physiol.* 90:1849–1854, 2001.
- ³⁵Ochoa, J. A., A. P. Sanders, D. A. Heck, and B. M. Hillberry. Stiffening of the femoral head due to inter-trabecular fluid and intraosseous pressure. *J. Biomech. Eng.* 113:259–262, 1991.
- ³⁶Ochoa, J. A., A. P. Sanders, T. W. Kiesler, D. A. Heck, J. P. Toombs, K. D. Brandt, and B. M. Hillberry. In vivo observations of hydraulic stiffening in the canine femoral head. *J. Biomech. Eng.* 119:103–108, 1997.
- ³⁷Porter, B., R. Zael, H. Stockman, R. Goldberg, and D. Fyhrie. 3-D computational modeling of media flow through scaffolds in a perfusion bioreactor. *J. Biomech.* 38:543–549, 2005.
- ³⁸Potier, E., J. Noailly, and K. Ito. Directing bone marrow-derived stromal cell function with mechanics. *J. Biomech.* 43:807–817, 2010.
- ³⁹Qin, Y. X., T. Kaplan, A. Saldanha, and C. Rubin. Fluid pressure gradients, arising from oscillations in intramedullary pressure, is correlated with the formation of bone and inhibition of intracortical porosity. *J. Biomech.* 36:1427–1437, 2003.
- ⁴⁰Qin, Y.-X., and H. Lam. Intramedullary pressure and matrix strain induced by oscillatory skeletal muscle stimulation and its potential in adaptation. *J. Biomech.* 42:140–145, 2009.
- ⁴¹Qin, Y.-X., W. Lin, and C. Rubin. The pathway of bone fluid flow as defined by in vivo intramedullary pressure and streaming potential measurements. *Ann. Biomed. Eng.* 30:693–702, 2002.
- ⁴²Riddle, R. C., and H. J. Donahue. From streaming-potentials to shear stress: 25 years of bone cell mechanotransduction. *J. Orthop. Res.* 27:143–149, 2009.
- ⁴³Rosen, C. J., and M. L. Boussein. Mechanisms of disease: is osteoporosis the obesity of bone? *Nat. Clin. Pract. Rheumatol.* 2:35–43, 2006.
- ⁴⁴Sandino, C., J. A. Planell, and D. Lacroix. A finite element study of mechanical stimuli in scaffolds for bone tissue engineering. *J. Biomech.* 41:1005–1014, 2008.
- ⁴⁵Schofield, R. The relationship between the spleen colony-forming cell and the haemopoietic stem cell. *Blood Cells* 4:7–25, 1978.
- ⁴⁶Sharp, L. A., Y. W. Lee, and A. S. Goldstein. Effect of low-frequency pulsatile flow on expression of osteoblastic genes by bone marrow stromal cells. *Ann. Biomed. Eng.* 37:445–453, 2009.

- ⁴⁷Teo, J. C. M., and S. H. Teoh. Permeability study of vertebral cancellous bone using micro-computational fluid dynamics. *Comput. Methods Biomech. Biomed. Eng.* 15:417–423, 2012.
- ⁴⁸Turner, C. H., and F. M. Pavalko. Mechanotransduction and functional response of the skeleton to physical stress: the mechanisms and mechanics of bone adaptation. *J. Orthop. Sci.* 3:346–355, 1998.
- ⁴⁹Vande Berg, B. C., J. Malghem, F. E. Lecouvet, and B. Maldague. Magnetic resonance imaging of the normal bone marrow. *Skeletal Radiol.* 27:471–483, 1998.
- ⁵⁰Watt, F. M., and B. L. Hogan. Out of Eden: stem cells and their niches. *Science* 287:1427–1430, 2000.
- ⁵¹Weisberg, S. P., D. McCann, M. Desai, M. Rosenbaum, R. L. Leibel, and A. W. Ferrante, Jr. Obesity is associated with macrophage accumulation in adipose tissue. *J. Clin. Invest.* 112:1796–1808, 2003.
- ⁵²White, F. M. *Fluid Mechanics*. New York: McGraw Hill, 1998.
- ⁵³White, D. R., H. Q. Woodard, and S. M. Hammond. Average soft-tissue and bone models for use in radiation dosimetry. *Br. J. Radiol.* 60:907–913, 1987.
- ⁵⁴Yeung, D. K. W., J. F. Griffith, G. E. Antonio, F. K. H. Lee, J. Woo, and P. C. Leung. Osteoporosis is associated with increased marrow fat content and decreased marrow fat unsaturation: a proton MR spectroscopy study. *J. Magn. Reson. Imaging* 22:279–285, 2005.
- ⁵⁵Yoo, A., and I. Jasiuk. Couple-stress moduli of a trabecular bone idealized as a 3D periodic cellular network. *J. Biomech.* 39:2241–2252, 2006.
- ⁵⁶Zhong, Z., and O. Akkus. Effects of age and shear rate on the rheological properties of human yellow bone marrow. *Biorheology* 48:89–97, 2011.